AFRL-HE-WP-JA-2006-0004

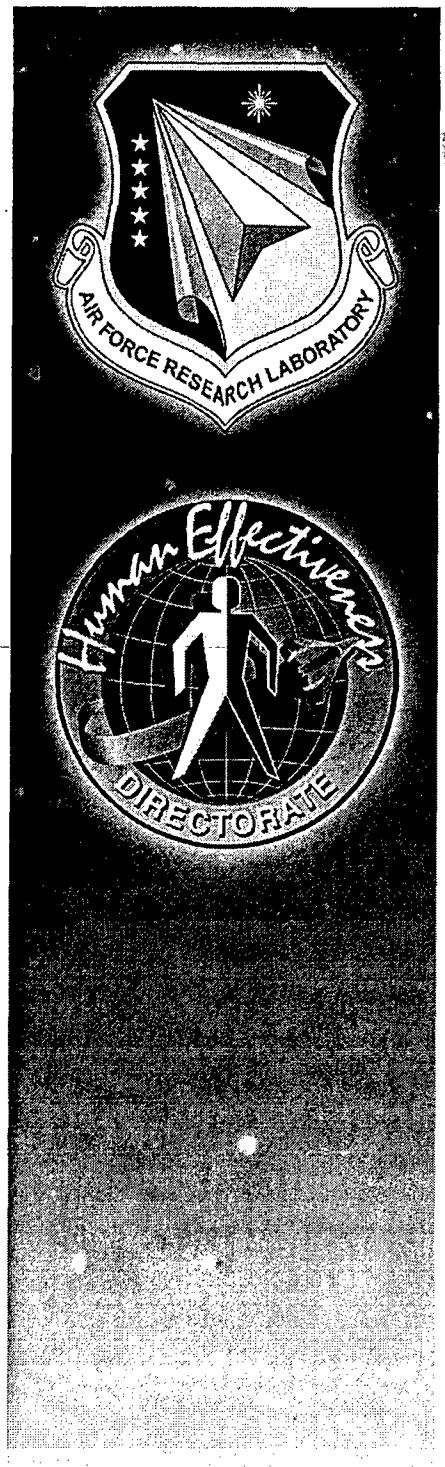

AIR FORCE RESEARCH LABORATORY

A Novel Approach for Predicting Human Response from ATD Tests

Zhiqing Cheng

Advanced Information Engineering Services
A General Dynamics Company

Joseph A. Pellettiere

Air Force Research Laboratory

May 2006

Interim Report for May 2004 to November 2004

Human Effectiveness Directorate
Biosciences and Protection Division
Biomechanics Branch
2800 Q Street, Bldg 824
Wright-Patterson AFB OH 45433-7947

REPORT DOCUMENTATION PAGE

Form Approved
OMB No. 0704-0188

1. REPORT DATE (DD-MM-YYYY)	2. REPORT TYPE	3. DATES COVERED (From - To)
May 2006	Interim	May 04 - Nov 04

4. TITLE AND SUBTITLE

A Novel Approach for Predicting Human Response from ATD Tests

5a. CONTRACT NUMBER
FA8650-04-D-6472

5b. GRANT NUMBER
N/A

5c. PROGRAM ELEMENT NUMBER
62202F

6. AUTHOR(S)

Zhiqing Cheng (AIES, General Dynamics)
Joseph A. Pellettiere (AFRL/HEPA)

5d. PROJECT NUMBER
7184

5e. TASK NUMBER
02

5f. WORK UNIT NUMBER
11

7. PERFORMING ORGANIZATION NAME(S) AND ADDRESS(ES) AND ADDRESS(ES)

Air Force Materiel Command
Air Force Research Laboratory, Human Effectiveness Directorate
Biosciences and Protection Division
Biomechanics Branch
Wright-Patterson AFB OH 45433-7947

8. PERFORMING ORGANIZATION REPORT NUMBER

AFRL-HE-WP-JA-2006-0004

9. SPONSORING / MONITORING AGENCY NAME(S) AND ADDRESS(ES)

10. SPONSOR/MONITOR'S ACRONYM(S)

AFRL/HEPA

11. SPONSOR/MONITOR'S REPORT NUMBER(S)

12. DISTRIBUTION / AVAILABILITY STATEMENT

Approved for public release; distribution is unlimited. Cleared by AFRL-WS-04-1444m 12/29/04.

13. SUPPLEMENTARY NOTES

Published in Stapp Car Crash Journal, Vol 48, Nov 2004

14. ABSTRACT

A methodology was developed for predicting the human response from ATD (Anthropomorphic Test Device) tests or for improving the biofidelity of the ATD response. The ATD response and human response are considered as the output of a black box system, from which the relationship between the ATD tests and human tests was established using wavelet analysis. Based on the decompositions of both responses on a wavelet packet basis, a mapping matrix is built after executing a procedure that includes de-noising and compression, energy distribution analysis, correlation analysis and regression analysis, and spectral coherence analysis and transfer function analysis. With the mapping matrix, an ATD response is modified or reconstructed into the corresponding human response. The practical use of the methodology was illustrated in the analysis of a series of lateral impact tests conducted on a horizontal impulse accelerator with an ATD and human volunteers as the test subjects. The predictions from the ATD tests using this method have attained significant improvement in biofidelity.

15. SUBJECT TERMS

ATD Tests, Human Tests, Wavelet Analysis, Wavelet Packet Analysis, Prediction, Modification

16. SECURITY CLASSIFICATION OF:			17. LIMITATION OF ABSTRACT	18. NUMBER OF PAGES	19a. NAME OF RESPONSIBLE PERSON
a. REPORT	b. ABSTRACT	c. THIS PAGE			Nathan Wright
U	U	U	SAR	19	19b. TELEPHONE NUMBER (include area code)

Standard Form 298 (Rev. 8-98)
Prescribed by ANSI Std. 239.18

Stapp Car Crash Journal, Vol. 48 (November 2004), pp.

A Novel Approach for Predicting Human Response from ATD Tests

Zhiqing Cheng
Advanced Information Engineering Services, A General Dynamics Company

Joseph A. Pellettiere
Human Effectiveness Directorate, Air Force Research Laboratory

ABSTRACT –A methodology was developed for predicting the human response from ATD (Anthropomorphic Test Device) tests or for improving the biofidelity of the ATD response. The ATD response and human response are considered as the output of a black box system, from which the relationship between the ATD tests and human tests was established using wavelet analysis. Based on the decompositions of both responses on a wavelet packet basis, a mapping matrix is built after executing a procedure that includes de-noising and compression, energy distribution analysis, correlation analysis and regression analysis, and spectral coherence analysis and transfer function analysis. With the mapping matrix, an ATD response is modified or reconstructed into the corresponding human response. The practical use of the methodology was illustrated in the analysis of a series of lateral impact tests conducted on a horizontal impulse accelerator with an ATD and human volunteers as the test subjects. The predictions from the ATD tests using this method have attained significant improvement in biofidelity.

KEYWORDS – ATD Tests, Human Tests, Wavelet Analysis, Wavelet Packet Analysis, Prediction, Modification

INTRODUCTION

Impact biomechanical tests play an important role in the studies of injury, crashworthiness, and safety. Since cadaver, animal and volunteer testing all carry with them potential ethical difficulties that can constrain the amount or type of testing that can be performed (Oakley 2001), Anthropomorphic Test Devices (ATDs), such as the Hybrid III manikin, have been widely used in the biomechanical tests. The development of ATDs has gone through a long process, and the biofidelity of ATDs has been improved along the process (Schneider et al. 1992; Kallieris et al. 1992; Viano et al. 1995). While an ATD is designed to mimic human response subject to impact, its biofidelity is often limited. As a consequence, biomechanical responses from the tests with ATDs and from the tests with human subjects are not always quite agreeable. Thus, a frequently asked question is how to predict human responses from an ATD test for the given biofidelity of the ATD; in other words, how can the biofidelity of the prediction of human response based on ATD tests be improved? The question is related to the relationship between the human tests and ATD tests.

A number of researches have been done on this subject or relevant topics. For instance, when a new ATD was introduced, a series of comparative tests were usually conducted to validate the biofidelity of the device by comparing the ATD's responses with the human's responses or cadaver's responses (Morgan et al. 1981; Seemann et al. 1986; Kallieris et al. 1992; Viano et al. 1995). Most of these studies were concerned with the assessment and evaluation of the performance of a device, with a few that addressed scaling or mapping an ATD response into a human response. Watkins and Guccione (1992) developed a technique for the scaling of the Hybrid III head kinematic response to the human head response when the subjects were under –Gx, +Gy, and +Gz impact acceleration. The scaling was based on the predictive equations that were established (identified) from actual data obtained from measurements taken using human volunteers and human surrogates exposed to the same accelerations, seat restraint, and test configurations. There are three steps in the scaling process: (1) Develop linear regression models for predicting human and surrogate response having appropriate parameters; (2) Reverse the surrogate model, i.e., develop the inverse

linear regression model to predict these common parameters from the surrogate response; (3) Insert these predicted parameters into the human response model and account for the non-common parameters by appropriate averaging.

In the Air Force Research Laboratory (AFRL), a number of series of tests have been performed over decades for evaluating the agreement between the human volunteer response and the ATD response under various impact conditions. These tests produced the data that can be used to establish the relationship between the human response and the ATD response for particular impact conditions. The relationship can be employed to improve the biofidelity of the prediction of human responses from ATD tests. The objective of this study is to develop a methodology for mapping an ATD response into the corresponding human response.

METHODS

Problem Statement and Analysis

The problem can be considered within a biomechanical system that consists of restraint systems (e.g., seat belts and airbags) and protection devices (e.g., floor padding and seat cushions), which are referred to as safety devices, and occupants. The system is characterized by the impact properties of the safety devices, the biomechanics of the occupants, and the interaction between the occupants and safety devices. The shock or impact to the occupant can be considered as an external disturbance to the system. The occupant response, a response of the system, depends upon the following factors:

- Impact conditions, which involve the magnitude (G-level), duration, and shape of the impact pulse; the manner in which the impact acts on the occupant (direction, location, and contact area); etc.
- Occupant biomechanics, which differ from a human and an ATD, even though an ATD is designed to have maximum biofidelity. The human biomechanics also differs among subjects, depending upon the gender, height, weight, and other anthropometric factors.
- Boundary conditions, which may include the airbag, seat belt or harness belt, seat cushion, helmet, face mask, and other restraints applied on the occupant, and the structures that surround the occupant and induce contact with the occupant.
- Initial conditions, which refer to the initial positioning of the occupant, pretensioning of the seat belt, etc.

The relationship between the human response and the ATD response will be considered only when both human and ATD are subject to the same or very similar impact conditions, boundary conditions, and initial conditions. Then we can reasonably judge that the discrepancy between the human response and the ATD response results from the differences in biomechanics between the human and the ATD. From the viewpoint of system analysis, problems of this kind are conventionally handled in terms of the transfer function of human, the transfer function of ATD, and the relationship between them. However, because of the complexity of a biomechanical system, the variety in impact conditions, boundary conditions, and initial states, and the nonlinearity of occupant biomechanics, it is not feasible or even possible to determine these transfer functions based on the input-output relationship of the system.

Alternatively, the problem could be tackled based on the occupant response only. Comparative tests between the human and the ATD are often performed for a range of conditions, and the human response and the ATD response are produced and acquired under the same conditions within the range. One idea is to consider the ATD response and human response as the output of a black box system and to establish the relationship between them via a signal analysis of them as a pair. This relationship can be used for the prediction of human response from the ATD tests, or, in other words, mapping the ATD response into human response, within the test range (interpolation) and out of the range (extrapolation) with certain restrictions.

Impact response, such as automobile crash response and seat ejection response, are transient, strongly localized in the time domain, and are often contaminated with noise. As a consequence, conventional statistical analysis, correlation analysis, or spectral analysis used for stationary signals may be neither appropriate nor efficient for the analysis of impact responses. As a new tool for signal analysis, wavelets are localized in both frequency and time domains, which match the major characteristics of transient impact responses. Therefore wavelets will be used in this study.

Introduction of Wavelet Analysis

In a wavelet basis, a signal $S(t)$ can be decomposed as (Strang and Nguyen 1997; Misiti et al. 1997)

$$\begin{aligned} S &= A_1 + D_1 \\ &= A_2 + D_2 + D_1 \\ &= \cdots \\ &= A_J + \sum_{j \le J} D_j \end{aligned}, \quad (1)$$

where

$$A_j(t) = \sum_k c_{jk}\, \phi_j(t-k), \quad (2)$$

and

$$D_j(t) = \sum_k d_{jk}\, \psi_j(t-k). \quad (3)$$

Here, A_j and D_j are referred to as the approximation and the detail of S at level j; $\phi_j(t)$ and $\psi_j(t)$ are the scaling function and the wavelet function at level j for reconstruction; and c_{jk} and d_{jk}, given by wavelet transforms, are scaling function coefficients and wavelet coefficients at level j and time shift k, respectively. Note that the decomposition of a signal using dyatic orthogonal wavelets is a quadratic sub-band filtering (Strang and Nguyen 1997). An ideal filter bank cuts the frequency band in half, but an actual filter bank has a transition band. However, it is true that the approximation and details are narrow-banded sub-signals of the original signal.

The total band is divided unevenly using a wavelet analysis. To obtain the decompositions over evenly spanned sub-bands, the wavelet packet analysis can be used (Strang and Nguyen 1997; Misiti et al. 1997). Wavelet packet analysis is a generalization of wavelet decomposition. In the orthogonal wavelet decomposition procedure, successive approximation coefficients are split into two parts, but successive details are never reanalyzed. In the corresponding wavelet packet situation, each detail coefficient vector is also decomposed into two parts using the same approach as in approximation vector splitting. This offers the richest analysis of a signal.

In a wavelet packet basis, the decomposition of the signal $S(t)$ at level j can be expressed as

$$S(t) = \sum_{n=0}^{2^j-1} \sum_k q_{jnk}\, w_{jn}(t-k), \quad (4)$$

where $w_{jn}(t)$ are wavelet packet atoms (Misiti el al. 1997); q_{jnk} are wavelet packet coefficients; n is the frequency index which is in accordance with the natural order of the nodes at this level; and k, the time shift, is the position index.

In wavelet packet analysis, for a J-level decomposition, from a complete wavelet packet decomposition tree there are more than $2^{2^{J-1}}$ different ways to encode a signal (Mallat 1998), for which a more general expression is

$$S(t) = \sum_{(j,n)\in I} \sum_k q_{jnk}\, w_{jn}(t-k), \quad (5)$$

where I is an index set which is chosen as

$$I = \{(j_0, n_0), (j_1, n_1), \ldots\}, \quad (6)$$

such that intervals $[2^{j_i} n_i, 2^{j_i}(n_i+1))$ are disjointed and cover the entire interval $[0,\infty)$ (Ogden 1997):

$$\bigcup_{i=0}^{\infty} [2^{j_i} n_i, 2^{j_i}(n_i+1)) = [0,\infty). \quad (7)$$

As the number of ways for the decomposition of a signal in wavelet packet bases may be very large and since explicit enumeration is generally unmanageable, it is necessary to find the optimal decomposition in terms of certain entropy criteria, computable by an efficient algorithm (Strang and Nguyen 1997; Misiti et al. 1997). These criteria include Shannon, Threshold, Norm, and Log Energy, which are available in the MATLAB wavelet toolbox (Misiti et al. 1997).

General Procedure

The entire procedure includes:

- Decomposing the response on a wavelet or wavelet packet basis.
- De-noising to remove noise and compressing to simplify the response representation.

- Decomposing both signals on a wavelet packet basis at the same level to get approximations and details (sub-signals).
- Energy distribution analysis of both signals to determine the energy contribution of each sub-signal.
- Correlation analysis between the two approximations and linear regression analysis between them to establish the relationship between them.
- Spectral coherence analysis or correlation analysis of a pair of sub-signals with significant energy contributions to determine the relationship between them. If linear relationship exists, determining the transfer function via FFT or scaling coefficient via regression.
- If linear relationship does not exist for the entire time duration, segmenting the sub-signals over evenly divided time spans. For a pair of segments with significant energy contributions, spectral coherence analysis or correlation analysis to determine the relationship between them. If linear relationship exists, determining the transfer function via FFT or scaling coefficient via regression.
- Summarizing the coefficients for the approximations and details to form the mapping matrix
- From the wavelet decompositions of the ATD response, with the mapping matrix, reconstructing the signal to obtain the prediction of human response.
- Statistical analysis for a range to obtain statistical parameters for the mapping matrix.

CASE STUDY AND RESULTS

Test Description

A series of tests were conducted at the AFRL using human subjects to investigate the effects of helmet inertial properties on the human response to short-duration sideward impacts of variable magnitude. The human subject population consisted of 24 male and 12 female volunteer subjects. All human subjects were members of the AFRL/HE Impact Acceleration Test Panel. The use of human testing in this program was approved by the AFRL Institutional Review Board (IRB) committee. The data of the tests can be found at http://www.biodyn.wpafb.af.mil with the Study No. of 199805. The data of the gender, height, weight, and sitting height of these test subjects, as well as their participation in each test, are given in Table 1.

The tests were performed on the Horizontal Impulse Accelerator (HIA), as shown in Figure 1. The sideward acceleration profile approximated a half-sine pulse with duration of 150 ms. The impact pulse was varied in magnitude at the level of 4, 5, and 6 g, respectively. The acceleration levels had been previously tested, and were proved to be well tolerated by the volunteer human subjects. Prior to human testing, tests were conducted at each test condition with an instrumented ATD (ADAM-L) that approximately corresponds to a 95th percentile male. Resulting test data reflect subject responses with ATD and humans at the same test conditions. These data will be used in the analyses in this paper

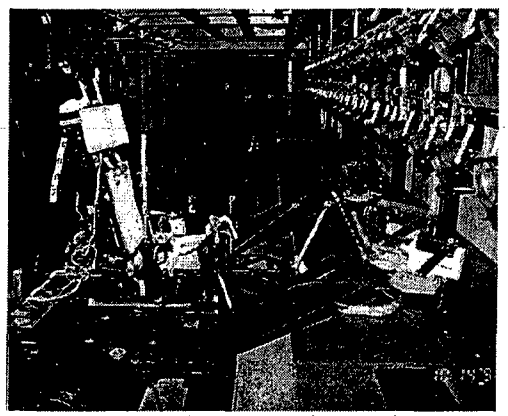

(a) AFRL Horizontal Impulse Accelerator

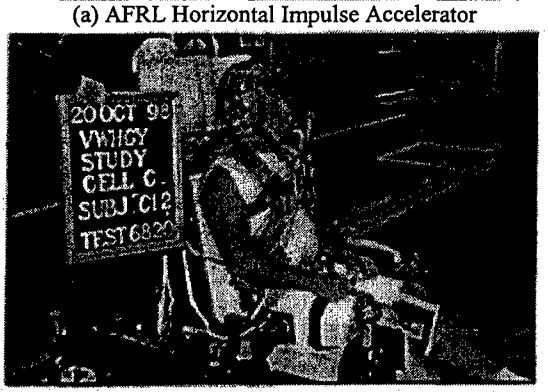

(b) Seating and initial position of occupant

Figure 1. Test setup

The measured electronic data included sled velocity and accelerations, seat accelerations, subject head and torso accelerations and displacements, and forces developed in the seat and the restraint system. The head accelerations were measured with a triaxial accelerometer array mounted on a bite bar. The bite bar accelerometer array also contained angular accelerometers to record rotational acceleration about the y-axis and the z-axis. Among the subject responses that were measured in the tests, the chest acceleration in the y-direction (lateral) (labeled as ChY in Figure 2), the head acceleration in the y-direction (HdY), the head angular acceleration about the y-axis (HdRy), and the head angular acceleration

about the z-axis (HdRz) are chosen for analysis, since they are the major responses to the side impact and are primarily concerned with injury.

For the ATD tests, standard 5^{th}, 50^{th}, and 95^{th} percentile ATDs are often used. But for the human tests, either female or male human subjects can vary in a large range of height, weight, and other anthropometric parameters, as was the case for this series of tests. Thus, in order to establish the correlative relationship between the ATD and human responses, the comparison between the ATD and human tests should not be on the one-to-one basis. Instead, it should be based on the one ATD to one human group match-up. Therefore, the human subjects are divided into three groups (which are small, medium, and large) according to weight, as shown in Table 2.

Table 1. The data of human test subjects

Subj. ID	Gender	Height (in)	Weight (lb)	Sitting Ht. (in)	Cell-A	Cell-B	Cell-C	Cell-D	Cell-E	Cell-F
B-11	M	73	233	37	x	x	x	x	x	x
B-16a	F	65.5	132	35.5	x	x	x	x	x	x
B-20	F	62	111	32	x					
B-21	M	70	190	37	x					
B-22	F	69.5	137	37	x	x	x	x	x	x
B-23	M	71.5	185	38	x	x	x	x	x	
B-24	M	70.5	195	39	x	x	x	x	x	x
B-25	F	64	143	33.8	x	x	x	x	x	x
B-26	M	73	155	36.3	x	x	x	x	x	x
B-9	M	69	161	34.5	x	x	x	x	x	x
C-12a	M	69	180	37	x	x	x	x	x	
C-17b	M	71	160	39	x	x	x	x	x	x
C-19	F	67	161	36	x	x	x	x	x	x
D-11	M	72	237	39	x	x	x	x	x	x
D-12	M	67	190	36.5	x	x	x	x	x	x
D-13	M	73	210	38.8	x	x	x	x	x	x
E-4	M	72.2	220	39	x	x	x	x	x	x
E-5	M	66	140	34	x	x	x	x	x	x
F-7	M	68	138	34	x					
H-13	M	70	160	36	x	x	x	x	x	x
H-16	M	68.8	180	36.5	x	x	x	x	x	x
H-18	M	74	250	38.5	x	x	x	x	x	
H-19	M	72	210	37.2	x	x	x	x	x	x
J-12	F	64	155	32.5	x	x				
J-7	M	68.5	160	36.5	x	x	x	x	x	x
L-11	F	65	130	34	x	x	x	x		
M-21b	M	66	150	34.5	x	x	x	x	x	x
M-32	F	66	134	34.5	x	x	x	x	x	
P-12	F	66	160	35.5	x	x	x	x		x
R-21	M	73	237	39	x	x	x	x		
S-11b	M	72	210	37.5	x	x	x	x	x	x
S-23	F	64.7	167	34.1	x	x	x	x	x	x
V-4	F	68	140	34.3	x	x				
W-11	F	64.5	140	35	x	x	x	x	x	x
W-12	M	69	180	36.5	x	x	x	x	x	x
Y-4	M	70	185	36	x	x	x	x	x	x

Table 2. Human subjects grouping

Gender	Small	Medium	Large
Female	<123.6 (lbs)	123.6~147.8 (lbs)	>147.8 (lbs)
Male	<155.7 (lbs)	155.7~188.1 (lbs)	>188.1 (lbs)

Table 3. Test Matrix

Test Cell	Sled Acc. (g)	Head Supported Weight (lbs)	Headrest Type
A	4	3.0	Contoured
B	5	3.0	Contoured
C	6	3.0	Contoured
D	5	0.0	Flat
E	5	0.0	Contoured
F	5	4.5	Contoured

The test matrix is shown in Table 3. In this series of tests, for each test cell, the ATD tests were repeated three times but the human subjects were tested only once.

Subject Responses

In the following analyses, ATD responses are the averaged results of three repeated tests, and human responses are the averaged results of all human subjects in each group (ML—Male Large; MM—Male Medium; MS—Male Small; FL—Female Large; FM—Female Medium; FS—Female Small). Figure 2, as an example, displays the subject responses in the ATD tests and the human tests under Cell A. The figure shows that whereas the agreement between the ATD tests and human tests is sound for the chest acceleration in the y-direction (ChY), the discrepancy between them is large for the head acceleration in the y-direction (HdY) and for the head angular accelerations about the y-axis (HdRy) and the z-axis (HdRz).

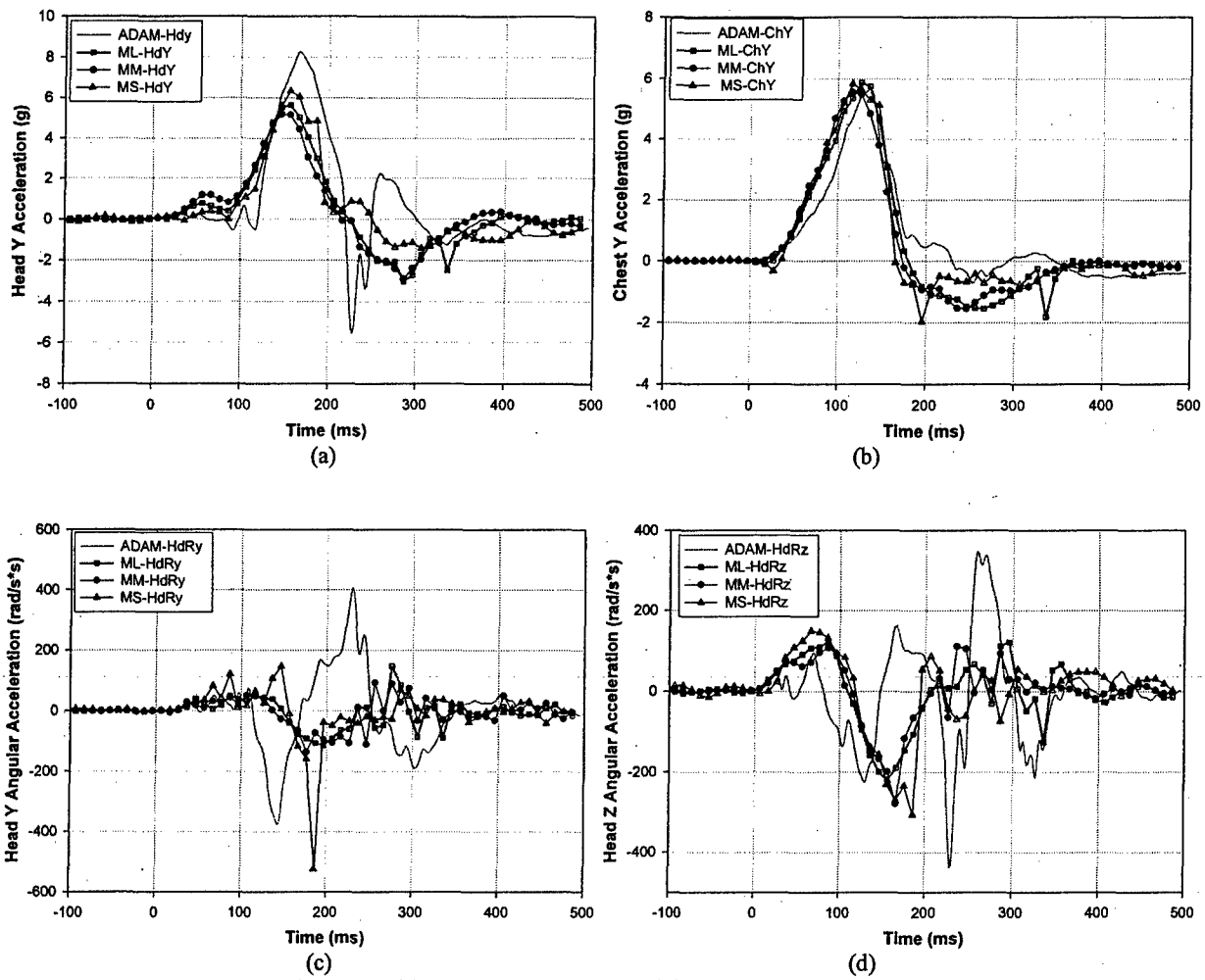

Figure 2. Subject responses of ATD and three male groups for Cell A

De-noising and Compression

The subject responses, treated as discrete digital signals, are analyzed using a wavelet packet. The fourth-order Daubechies wavelet packet is chosen for the analyses (Daubechies 1997; Misiti et al. 1997). The decomposition level is chosen such that the sub-signal at the first node at this level, which represents the approximation of the original signal, basically describes the gross motion of the occupant at the corresponding location. Whereas trial analysis at different levels can reveal the underlying gross motion of a response, subjective judgment may be required. Through trial analysis, it is found that an appropriate decomposition level for the chest acceleration is 5 and for the three head responses is 6.

The signals are decomposed on the selected wavelet packet (db4) basis. The best decomposition is performed using the entropy criterion. Then, the de-noised version of the original signal is obtained by soft thresholding of wavelet packet coefficients (Misiti et al. 1997). De-noising removes the noise from a signal and thus reduces the energy contained in the signal. The de-noised signal is decomposed on the best decomposition tree again according to the chosen entropy criterion. Compression, by hard thresholding of wavelet packet decomposition coefficients, is performed to simplify the representation of the de-noised signal. The compression replaces insignificant coefficients with zero and thus removes the energy associated with these coefficients (Misiti et al. 1997).

As illustrations, for the subject responses from ATD tests and human tests of the large male group (ML) and large female group (FL), the original signals, and the de-noised and compressed signals are displayed in Figures 3-6. As a preparation step in the entire procedure, de-noising and especially compression are not necessary if the original signal is "clean." Whereas the signal energy can be well retained through compression, the peak value of a signal may have significant change, as shown in Fig. 3 (a), since some coefficients are zeroed out by hard thresholding.

Decomposition

In the wavelet packet analysis, there are various ways to encode a signal, as indicated by Eq. (5). In order to obtain the decompositions over evenly spanned sub-bands and to provide a common basis, $S_{1c}(t)$ and $S_{2c}(t)$, the de-noised and compressed versions of the two original signals, $S_1(t)$ and $S_2(t)$, will be decomposed on the same wavelet packet and at the same level. That is, from Eq. (4),

$$S_{1c}(t) = \sum_{n=0}^{2^j-1} \sum_{k} q_{jnk_1} w_{jn}(t-k)$$
$$S_{2c}(t) = \sum_{n=0}^{2^j-1} \sum_{k} q_{jnk_2} w_{jn}(t-k) \quad , \qquad (8)$$

where the level j is chosen in the same manner as that used in de-noising and compression, that is, the sub-signal at the first node of this level, which is the approximation of the original signal, represents the gross motion of the occupant at the corresponding location.

The de-noised and compressed signals are decomposed on the db4 wavelet packet basis at level 5 for the chest acceleration and level 6 for the head accelerations. For the decomposition at level 5, there are 32 terminal nodes ($n = 0, 1, \cdots, 31$), and for that at level 6 there are 64 terminal nodes ($n = 0, 1, \cdots, 63$).

Energy Distribution

For each de-noised and compressed signal, the energy distribution with respect to the node order n (related to the frequency band) and time position k (Cheng et al. 2004) are calculated. For the subject responses from the ATD tests and the human tests of the large male group (ML) and the large female group (FL), the energy distributions of the de-noised and compressed signals are displayed in Figures 3-6 also. These figures show that the major energy of these responses is contained in the first node. This means that the approximation or gross motion of each response is the dominant component. The distribution of the energy contained in each node (frequency band) over the time spans can be intuitively viewed also. Based on the energy distribution, the sub-signals (the approximation at the first node and the details at the higher-order nodes) with significant energy can be identified, and those with insignificant energy can be eliminated. This will help us to focus on those significant components of a response.

Mapping of Approximations

The approximations of the ATD response and the human response can be treated as deterministic or narrow-banded signals, and thus the conventional correlation analysis can be used to determine the relationship between them (Cheng and Pellettiere 2003). Since the peak-timing difference or time shift may exist between the two approximations, the maximum absolute value of correlation coefficient is searched in a range of time shift. Thus obtained

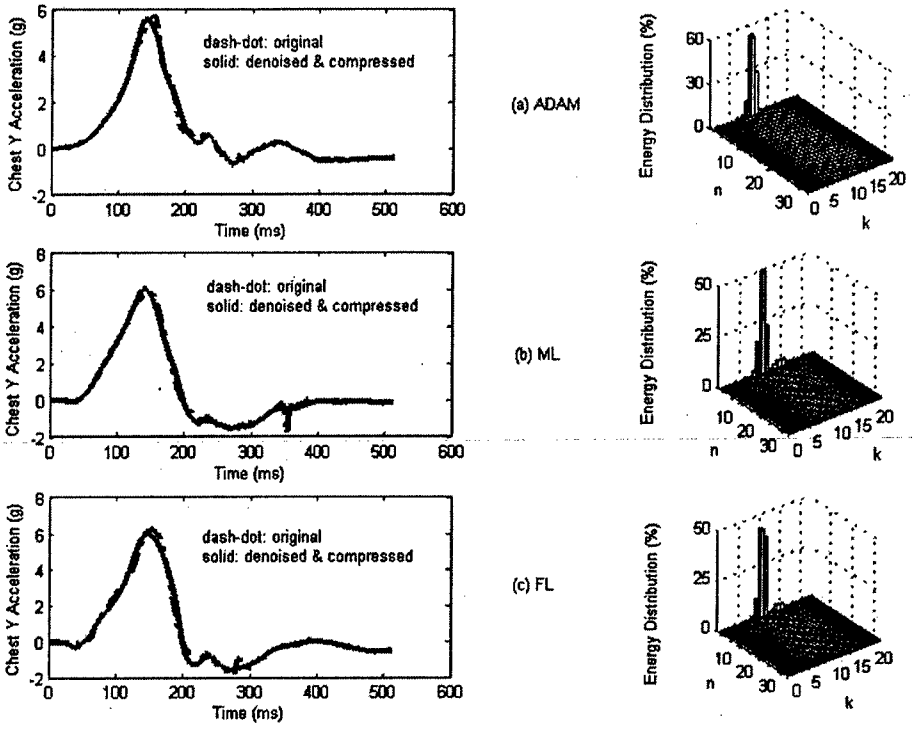

Figure 3. De-noising, compression, and energy distribution of chest y acceleration for Cell A

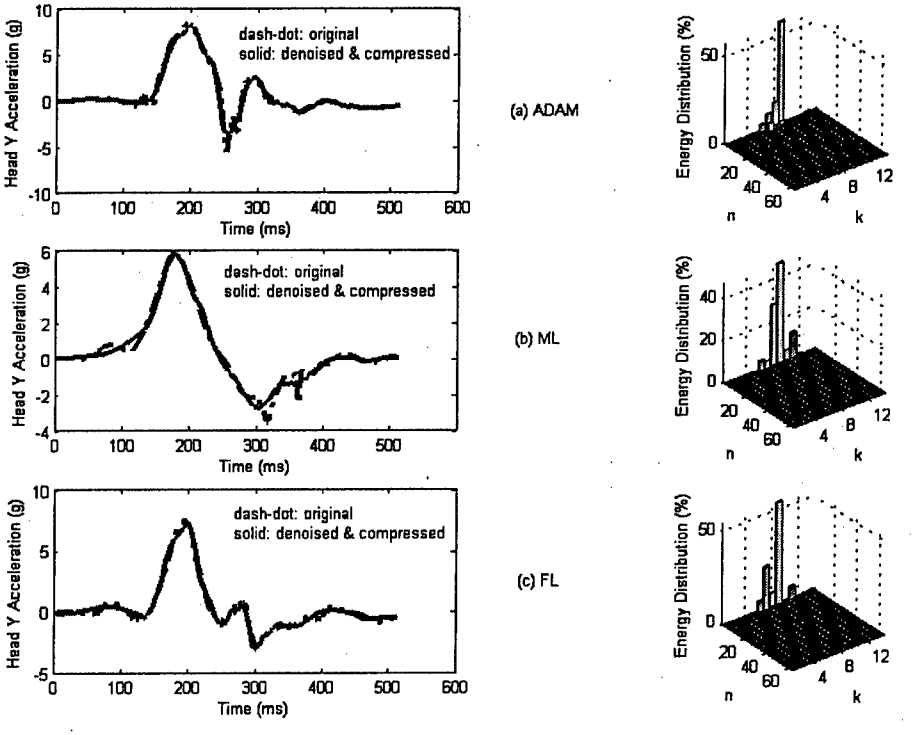

Figure 4. De-noising, compression, and energy distribution of head y acceleration for Cell A

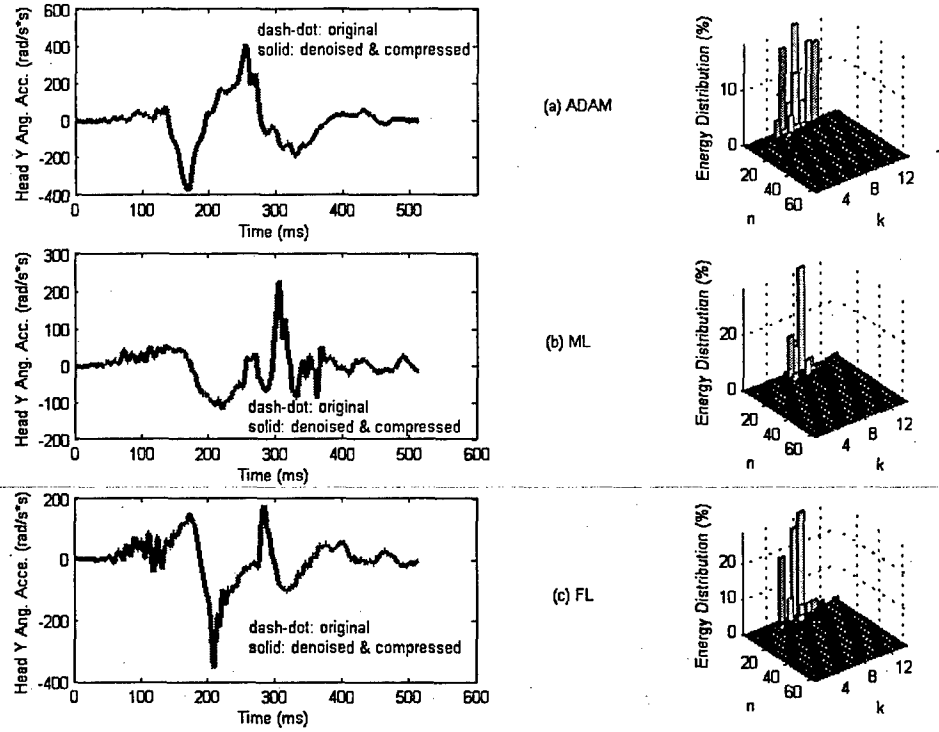

Figure 5. De-noising, compression, and energy distribution of head y angular acceleration for Cell A

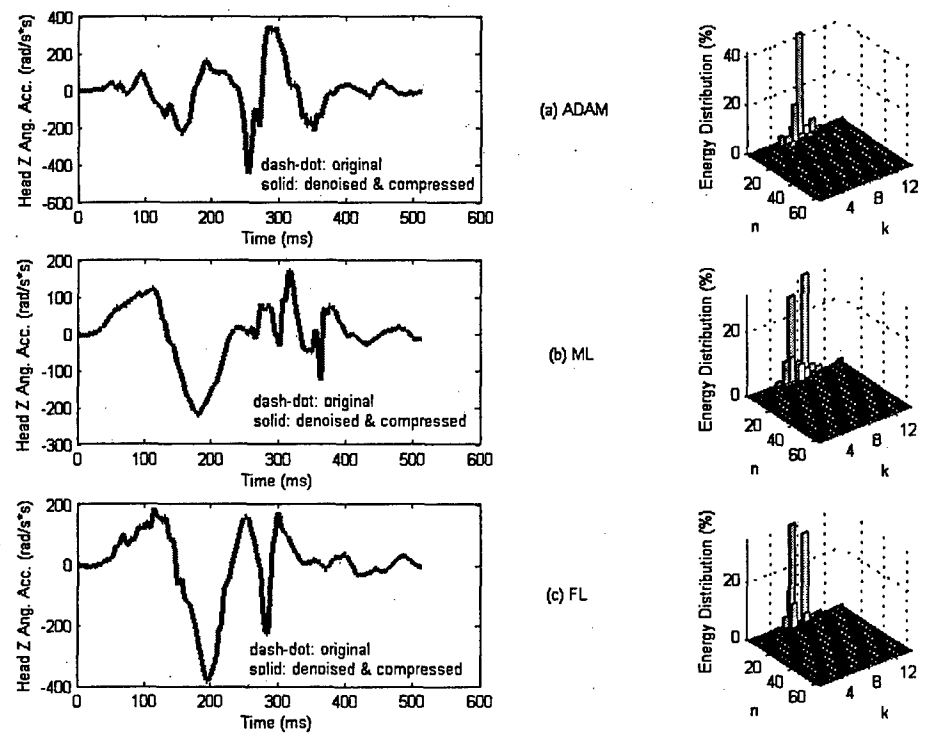

Figure 6. De-noising, compression, and energy distribution of head z angular acceleration for Cell A

correlation coefficient ρ_a and the corresponding time shift τ_0 are given in Table 4 for the large male group and in Table 5 for the large female group, which represent the relationship between the ATD responses and the corresponding human responses in terms of their gross motions. The calculated scaling factor k_a is given in Tables 4 and 5 also. Together with the time shift τ_0, the scaling factor k_a can be used to map the approximation of an ATD response into the approximation of the counter human response. Figures 7 and 8 illustrate the mapping of approximations from ATD responses into human responses for the large male group (Figure 7) and for the large female group (Figure 8) under Cell C.

In Tables 4 and 5, three test cells are covered. These test cells define a range of impact level from 4 to 6 g. The averages of scaling factor k_a and time shift τ_0 over the three cells can be used for the mapping of approximations of the ATD responses into the corresponding human responses in this range. The averaged values of k_a and τ_0 are given in Tables 4 and 5.

Mapping of Details

In wavelet packet analysis, the decomposition at the first node ($n = 0$) corresponds to the approximation in wavelet analysis at the same level, while the decompositions at all other terminal nodes ($n > 0$) correspond to the details in wavelet analysis. From Eq. (4), the decompositions of $S_1(t)$ and $S_2(t)$ at each node, denoted as $S_{1dn}(t)$ and $S_{2dn}(t)$, respectively, are given by

$$S_{1dn}(t) = \sum_k q_{jnk_1} w_{jn}(t-k)$$
$$S_{2dn}(t) = \sum_k q_{jnk_2} w_{jn}(t-k) \quad (9)$$

which can be considered as a sub-signal of the original signal in a particular frequency band associated with each node. Often, these sub-signals are cyclic and can be considered as narrow-banded vibration signals. Therefore, for a pair of sub-signals $\{S_{1dn}(t), S_{2dn}(t)\}$ of the original ATD and human responses $\{S_1(t), S_2(t)\}$, spectral coherence analysis (Bendat and Piersol 1993) can be used to determine the relationship between them. If the relationship is linear, the transfer function can be identified from spectral analysis and used to map the details of the ATD's response into the details of the human response.

In this series of tests, the ATD tests were repeated three times at each test cell, so that the sample size $n_d = 3$. Each human subject was tested only once for each test cell, so that for each human subject $n_d = 1$. However, if human tests are considered in a group, each group has several subjects. If the differences in biomechanical characteristics among the subjects in a group are not significant and thus can be neglected, the sample size is the number of the subjects in the group. However, as shown in the tests, the differences are not trivial, so the averaged response is used for each human group in this study. This means that for each human group, $n_d = 1$. Note that the results of spectral coherence analysis are meaningless if $n_d = 1$ (Bendat and Piersol 1993). Therefore, spectral coherence analysis is not applicable in this case study.

Alternatively, the relationship between an ATD response and the counter human response for the details can be based on correlation analysis. Since the details are often strongly localized in time domain, they may not be well correlated in the entire time duration. However, the two sub-signals are probably related to each other in certain time spans. Therefore, the sub-signals at each node can be further divided into segments that are defined in subintervals of time so that local characteristics can be investigated (Cheng and Pellettiere, 2003).

The correlative relationship between the two segments (one is from the ATD, and the other is from the human) is determined using conventional correlation analysis. If the relationship is linear, linear regresion analysis is used to obtain the scaling factor k_d, which is used to map this segment of the detail of the ATD response into the counter one of the human response. As an illustration, the mapping matrix used for the mapping of the details from the ADAM-L's response into the large female's response for the head z angular acceleration in Cell C is given in Table 6. There are 64 nodes at this level (level 6). The segment length is chosen to be 64 (data points). Since the total length of a sginal is 512 (data points), there are 8 segments for each node. Note that the coefficients for N>30 are zero. This is because the energy contained in these higher order nodes is insignificant.

Table 4. Scaling factor and time delay for large male group

Test Cell	Cell A			Cell B			Cell C			Average	
Subject	ρ_a	τ_0	k_a	ρ_a	τ_0	k_a	ρ_a	τ_0	k_a	τ_0	k_a
ML-Cy	0.949	-7	1.173	0.971	-20	1.309	0.958	-13	1.197	-13	1.226
ML-Hy	0.893	-17	0.831	0.516	-20	0.539	0.769	-20	0.776	-19	0.715
ML-HRy	0.682	-20	-0.270	0.418	-20	-0.112	0.659	-10	-0.252	-17	-0.211
ML-HRz	0.682	20	0.921	0.717	11	0.463	0.768	10	0.644	14	0.676

Table 5. Scaling factor and time delay for large female group

Test Cell	Cell A			Cell B			Cell C			Average	
Subject	ρ_a	τ_0	k_a	ρ_a	τ_0	k_a	ρ_a	τ_0	k_a	τ_0	k_a
FL-Cy	0.954	2	1.196	0.958	-18	1.139	0.973	-17	1.108	-11	1.148
FL-Hy	0.954	-4	0.795	0.393	-20	0.354	0.693	-20	0.634	-15	0.594
FL-HRy	0.560	-20	-0.360	0.540	-20	-0.179	0.466	-20	-0.157	-20	-0.232
FL-HRz	0.494	20	0.779	0.839	7	0.683	0.904	8	0.879	12	0.780

Table 6 A mapping matrix for details (Large female group, head z angular acceleration, Cell C)

	Segment No.								Node No.	Segment No.							
Node No.	1	2	3	4	5	6	7	8		1	2	3	4	5	6	7	8
0	0.00	0.00	0.00	0.00	0.00	0.00	0.00	0.00	32	0.00	0.00	0.00	0.00	0.00	0.00	0.00	0.00
1	4.61	0.00	-2.24	0.00	-0.26	-0.09	0.00	0.00	33	0.00	0.00	0.00	0.00	0.00	0.00	0.00	0.00
2	0.00	-0.25	-0.91	-0.85	-1.23	0.00	0.00	-0.52	34	0.00	0.00	0.00	0.00	0.00	0.00	0.00	0.00
3	0.00	0.00	0.00	1.65	1.03	-0.43	-0.55	0.00	35	0.00	0.00	0.00	0.00	0.00	0.00	0.00	0.00
4	-0.12	-0.15	-0.24	0.00	-1.82	-1.72	0.00	-1.14	36	0.00	0.00	0.00	0.00	0.00	0.00	0.00	0.00
5	0.00	-0.46	-1.19	-2.46	0.71	0.78	0.99	1.31	37	0.00	0.00	0.00	0.00	0.00	0.00	0.00	0.00
6	0.16	0.00	0.00	0.00	0.00	-1.26	1.08	-0.26	38	0.00	0.00	0.00	0.00	0.00	0.00	0.00	0.00
7	0.00	0.42	-0.59	0.00	0.67	0.30	0.00	-1.49	39	0.00	0.00	0.00	0.00	0.00	0.00	0.00	0.00
8	0.25	-0.87	0.00	0.00	0.00	-0.39	-0.40	-0.19	40	0.00	0.00	0.00	0.00	0.00	0.00	0.00	0.00
9	0.47	0.93	0.27	0.16	0.19	0.00	-0.20	0.00	41	0.00	0.00	0.00	0.00	0.00	0.00	0.00	0.00
10	5.00	0.00	0.00	0.00	0.00	-0.28	0.55	-0.86	42	0.00	0.00	0.00	0.00	0.00	0.00	0.00	0.00
11	1.80	1.40	0.00	0.43	0.62	0.00	0.00	0.00	43	0.00	0.00	0.00	0.00	0.00	0.00	0.00	0.00
12	-9.77	0.00	0.00	-0.41	0.00	1.61	0.00	0.00	44	0.00	0.00	0.00	0.00	0.00	0.00	0.00	0.00
13	-2.18	0.00	0.31	0.00	0.00	0.00	0.00	0.00	45	0.00	0.00	0.00	0.00	0.00	0.00	0.00	0.00
14	0.00	0.00	-4.31	0.00	0.00	0.47	0.00	-1.49	46	0.00	0.00	0.00	0.00	0.00	0.00	0.00	0.00
15	8.95	0.00	0.00	0.00	0.00	-0.68	-0.65	-1.05	47	0.00	0.00	0.00	0.00	0.00	0.00	0.00	0.00
16	0.00	0.00	0.00	0.00	0.00	0.00	0.00	0.00	48	0.00	0.00	0.00	0.00	0.00	0.00	0.00	0.00
17	0.00	0.00	0.00	0.00	0.00	0.00	0.00	0.00	49	0.00	0.00	0.00	0.00	0.00	0.00	0.00	0.00
18	0.00	0.00	0.00	0.00	0.00	0.00	0.00	0.00	50	0.00	0.00	0.00	0.00	0.00	0.00	0.00	0.00
19	0.00	0.00	0.00	0.00	0.00	0.00	0.00	0.00	51	0.00	0.00	0.00	0.00	0.00	0.00	0.00	0.00
20	0.00	0.00	0.00	0.00	0.00	0.00	0.00	0.00	52	0.00	0.00	0.00	0.00	0.00	0.00	0.00	0.00
21	0.00	0.00	0.00	0.00	0.00	0.00	0.00	0.00	53	0.00	0.00	0.00	0.00	0.00	0.00	0.00	0.00
22	0.00	0.00	0.00	0.00	0.00	0.00	0.00	0.00	54	0.00	0.00	0.00	0.00	0.00	0.00	0.00	0.00
23	0.00	0.00	0.00	0.00	0.00	0.00	0.00	0.00	55	0.00	0.00	0.00	0.00	0.00	0.00	0.00	0.00
24	-0.11	0.00	-1.40	2.01	0.00	9.77	27.77	0.00	56	0.00	0.00	0.00	0.00	0.00	0.00	0.00	0.00
25	0.00	0.00	0.00	1.00	3.31	-7.93	0.00	0.00	57	0.00	0.00	0.00	0.00	0.00	0.00	0.00	0.00
26	0.00	0.00	0.00	0.00	0.00	0.00	0.00	0.00	58	0.00	0.00	0.00	0.00	0.00	0.00	0.00	0.00
27	0.00	0.00	0.00	0.00	0.00	0.00	0.00	0.00	59	0.00	0.00	0.00	0.00	0.00	0.00	0.00	0.00
28	0.00	0.00	0.00	0.00	0.00	0.00	0.00	0.00	60	0.00	0.00	0.00	0.00	0.00	0.00	0.00	0.00
29	0.00	0.00	0.00	0.00	0.00	0.00	0.00	0.00	61	0.00	0.00	0.00	0.00	0.00	0.00	0.00	0.00
30	0.00	0.00	-0.85	-0.34	0.00	-5.34	0.00	-31.72	62	0.00	0.00	0.00	0.00	0.00	0.00	0.00	0.00
31	0.00	0.00	0.00	0.00	0.00	0.00	0.00	0.00	63	0.00	0.00	0.00	0.00	0.00	0.00	0.00	0.00

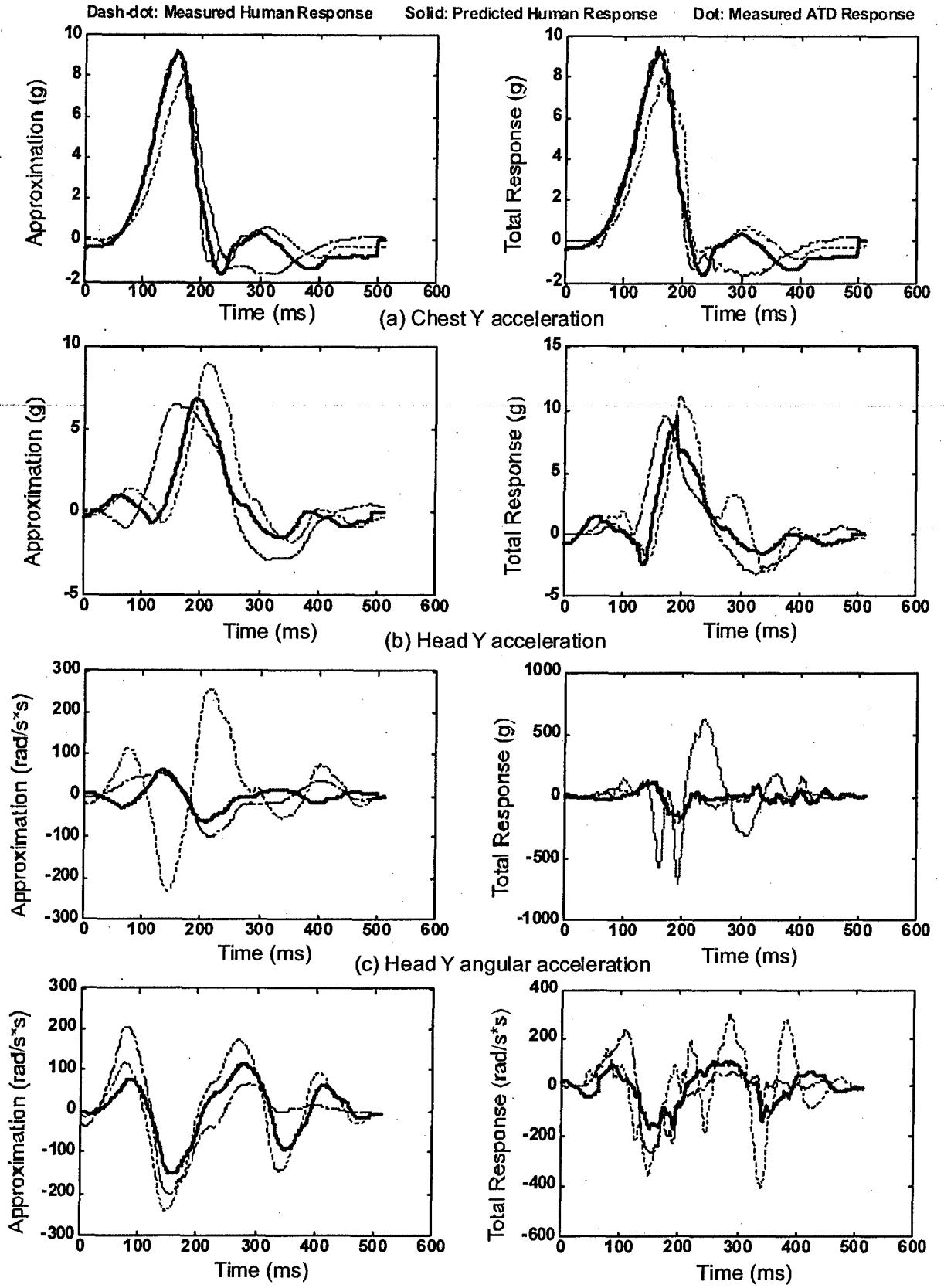

Figure 7. Mapping and synthesizing for large male group under Cell C

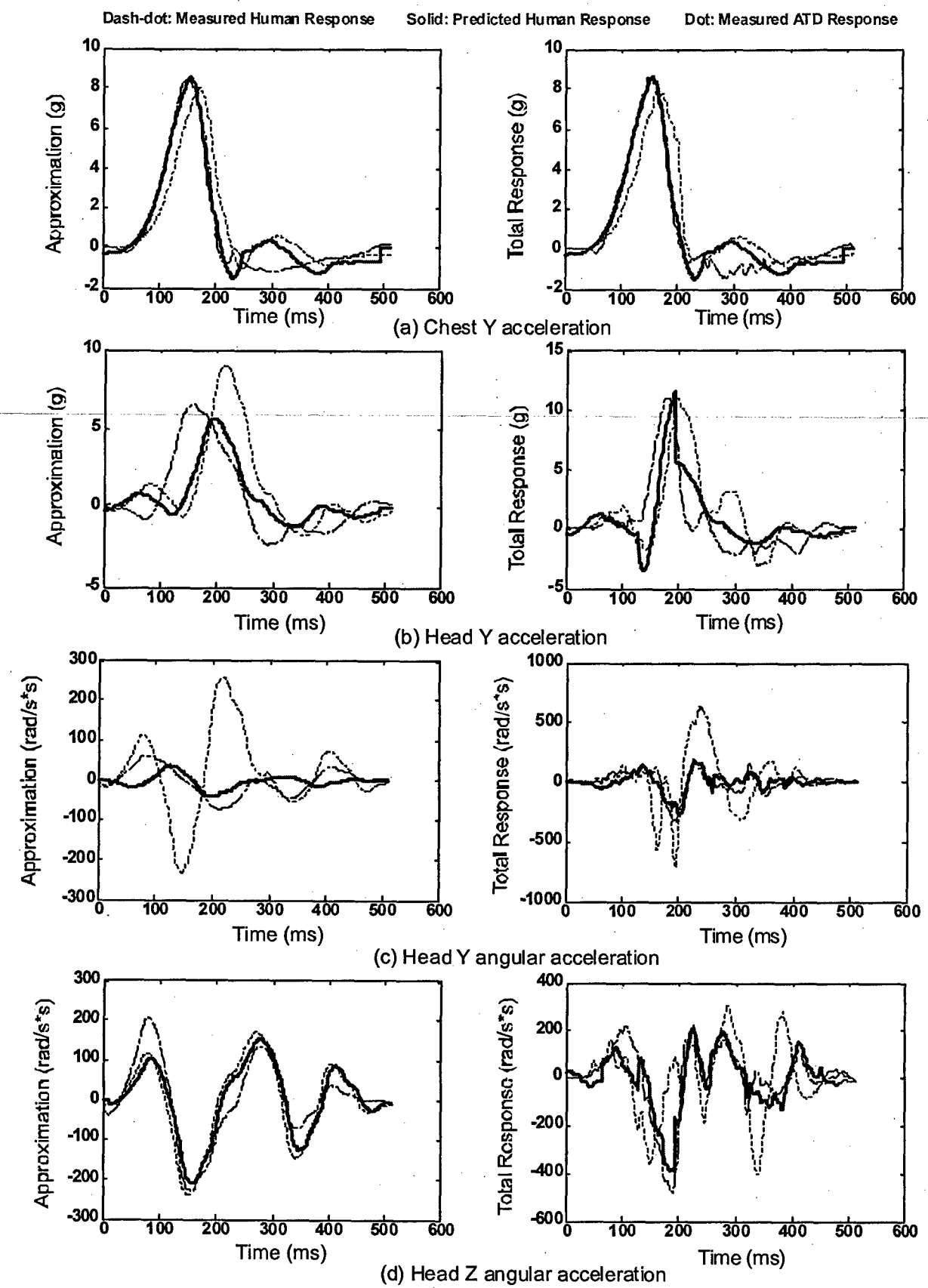

Figure 8. Mapping and synthesizing for large female group under Cell C

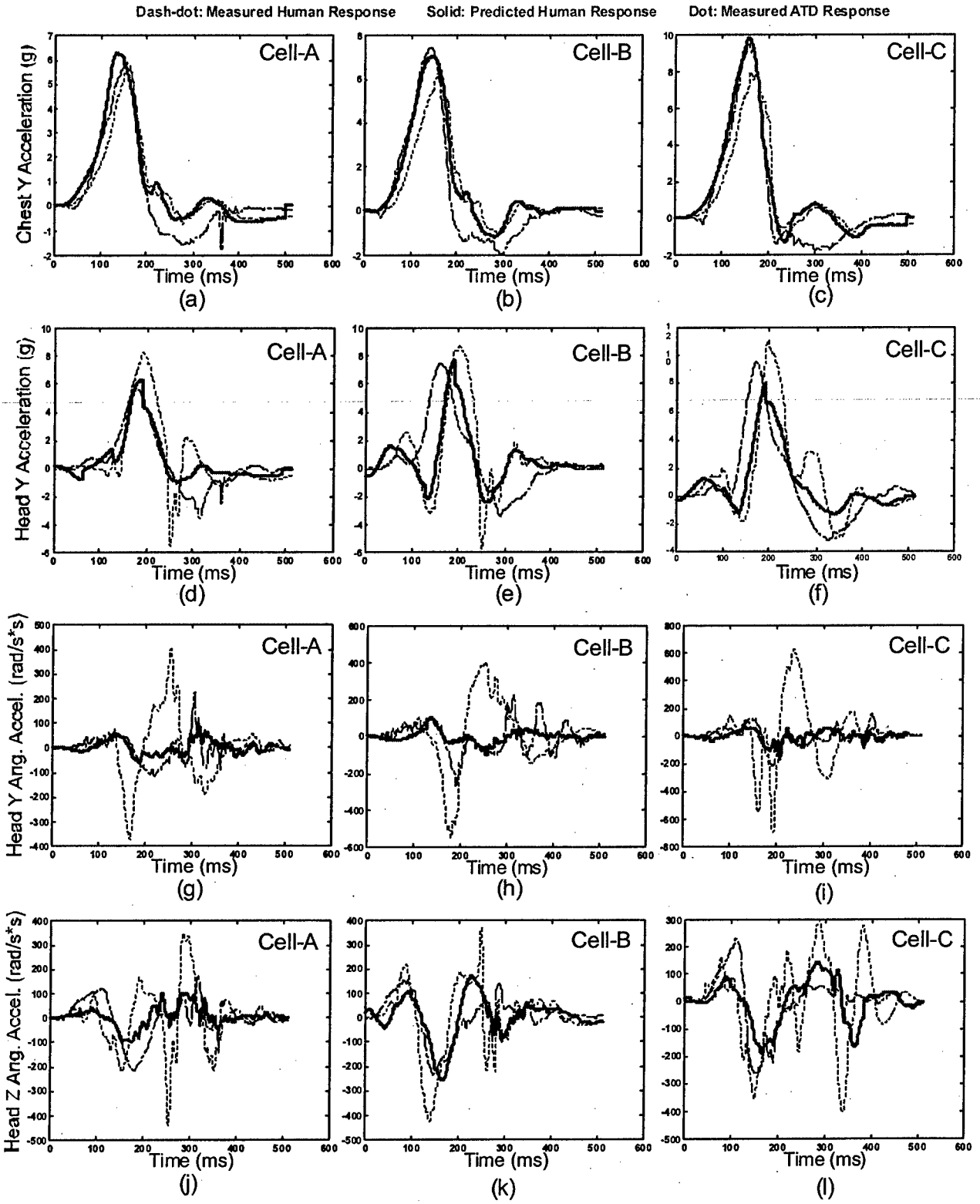

Figure 9. Prediction for large male group in the range of three cells

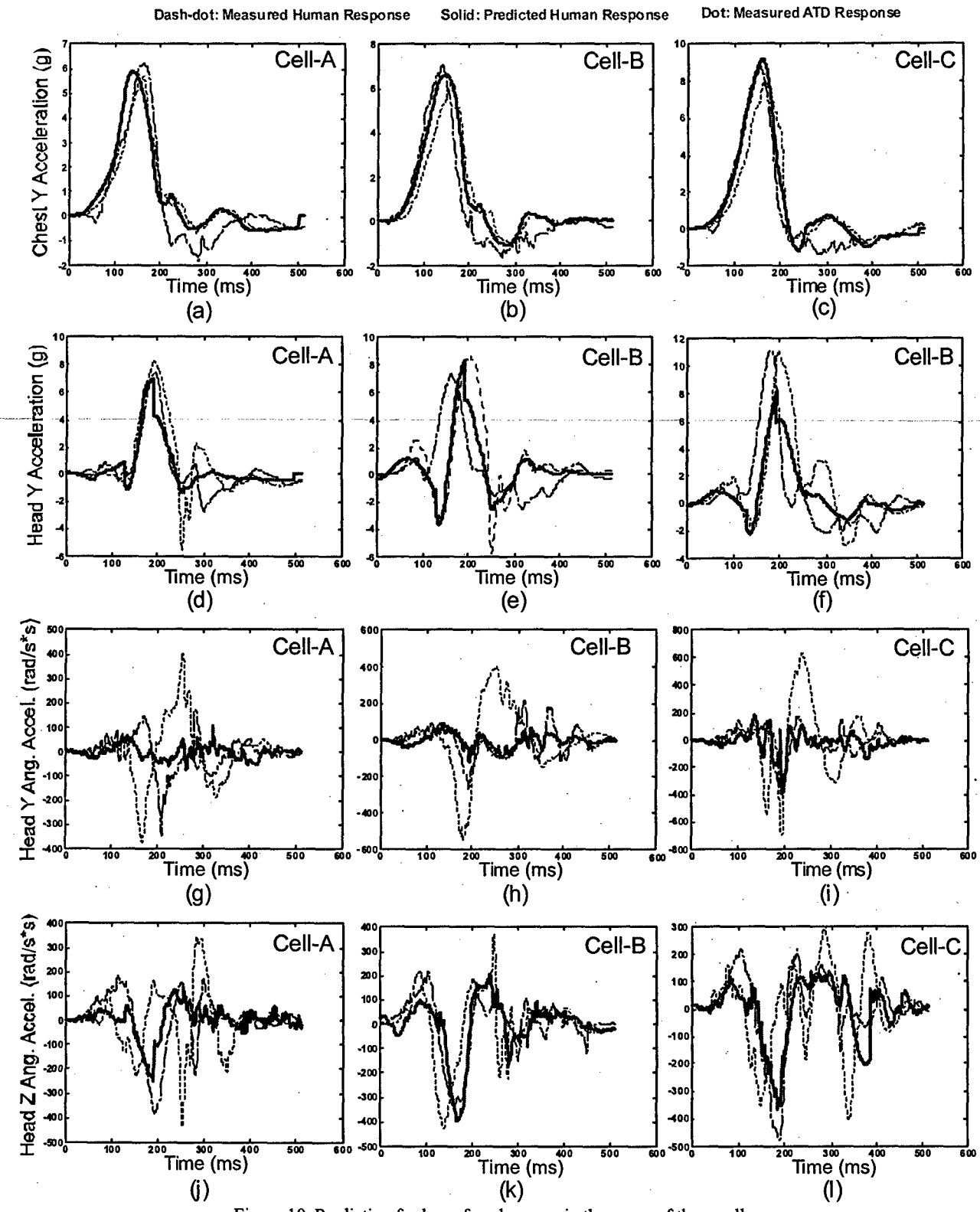

Figure 10. Prediction for large female group in the range of three cells

Synthesizing Total Response

The total response for a human is obtained by synthesizing the approximation and the details that are mapped from the corresponding ATD response. Figures 7 and 8 illustrate the synthesized total responses for the large male group and the large female group under the test conditions of Cell C. The human responses and the ATD responses that were measured from the tests are also displayed in the figures for comparison.

Prediction of Human Response

Based on the established relationship or mapping matrix between the ATD responses and the human responses, the human responses can be predicted from the ATD tests. The prediction can be made for a test cell or for a range that is defined by several test cells. When the prediction is to be made for a specific test cell, the relationship or mapping matrix established for that cell should be used, since it provides a better description of the relationship under the conditions of that cell than the general mapping matrix that is developed for the entire range. Figures 7 and 8 display the predicted human responses for Cell C with the mapping matrix developed for this cell. The prediction in a range (defined by three test cells) is shown in Figures 9 and 10 for the large male group and the large female group. The general relationship or mapping matrix for this range, which is generated from the averaging of the mapping matrices for the three test cells, is used for the prediction for each test cell.

DISCUSSION

Effectiveness in Improvement

The practical application of the method has been illustrated in the analysis of the HIA tests described above, which provides the results that can be used to evaluate the effectiveness of the method. Figures 7-10 show that overall, compared to the original ATD responses, their mappings or the predicted human responses get closer to the measured human responses. The closeness of the predicted human responses to their measured ones varies from the chest accelerations to the other three head accelerations. The closeness depends on the correlation coefficients between the approximations of the ATD and human responses, because the approximations are the dominant or major components of respective responses. From Tables 4 and 5 and Figures 7 and 8, it can be observed that the higher the correlation between the approximations of the ATD response and the human response, the closer the predicted human response to the measured one. In this sense, the correlation coefficient between the approximations describes the degree of the biofidelity of the ATD in the representation of respective human response.

On the contrary, improvement of the prediction by this method increases from the chest acceleration to the head accelerations. As shown in Figures 7-10, whereas the improvement of the prediction by this method is not quite pronounced for the chest acceleration, it is remarkably significant for the head angular accelerations, even though the correlative coefficients between the approximations of the ATD and human responses are low. This is because for the head angular accelerations, the approximations are less dominant and the details are more significant. The mapping of the details contributes to the improvement of the prediction.

The validity of the prediction also depends upon whether the prediction is made for a case or for a range. When the prediction is to be made for a case, the mapping relationship established for this case is used. When the prediction is to be made for a range, the general mapping relationship established for the range is used, which is developed from the mapping relationships of all cases in this range. Theoretically, the mapping relationship established for each individual case provides the best description for each respective case, so that in general, for a particular case, the prediction using the mapping matrix for this case will be better than the prediction using the general mapping relationship. This can be verified by the comparison of Figures 7 and 8 to Figures 9 and 10.

Using the general mapping relationship in the prediction for a particular case may result in degradation rather than improvement, as shown in Figure 10 (f). The problem is due to the time shift between the measured ATD and human responses. The prediction for the Cell C (Figure 10 (f)) is based on the general mapping relationship that is the average of the three respective mapping matrices for Cell A (Figure 10 (d)), Cell B (Figure 10 (e)), and Cell C. However, the time shift for Cell A (Figure 10 (d)) is small whereas the time shift for Cell B and Cell C are very large. In the computation of the correlation coefficients given in Table 5, the time shift is confined to the range of (-20, 20) Δt for all accelerations; but the actual time shift between the ATD response and the human response is much larger for Cell B and Cell C, as shown in Table 7. This indicates that the results of these three tests (Cell A, Cell B, and Cell C) are not consistent. The prediction with the averaged values of τ_0 and k_a given in Table 7 are still not satisfactory.

Table 7. Scaling factor and time delay for large female group

Test Cell	Cell A			Cell B			Cell C			Average	
Subject	ρ_a	τ_0	k_a	ρ_a	τ_0	k_a	ρ_a	τ_0	k_a	τ_0	k_a
FL-Hy	0.954	-4	0.795	0.719	-57	0.650	0.949	-56	0.873	-39	0.773

The problem induces concerns with the building and implementation of a general mapping matrix. Certain pre-analysis and processing are necessary to ensure that the test conditions are fully controlled and the tests results are consistent, to identify "wild" cases, and to eliminate them from the test matrix. If the results of all tests are consistent but have significant variations, the simple averaging is not a good way to build the general mapping relationship. More sophisticated analysis and processing need to be implemented in the building of the general mapping matrix so as to reveal the trend underlying those variations

Selection of Wavelets or Wavelet Packets

Wavelets or wavelet packets are used as the foundation of the methodology. Unlike the Fourier analysis where only sinusoidal waveform is used, the wavelet analysis can be performed with various waveforms (wavelet functions). The selection of an appropriate wavelet function is important and may affect the effectiveness of the methodology. A general rule is not available, but several factors may be involved in the selection and need to be considered (Misiti et al. 1997):

- Orthogonality, required for the energy distribution analysis;
- Finite support width, needs to be reasonably small in order to catch the abrupt changing features of impact signals;
- Exact reconstruction, required for the prediction;
- Fast algorithm, preferred for large volume data.

Whereas different wavelets form different bases on which the decomposition of a signal may be different and thus the mapping matrix may be different, the final result, i.e., prediction, should be unique. This is because the selected wavelets have perfect (exact) reconstruction (Strang and Nguyen 1997; Daubechies 1997).

Robustness

Since this method is based on wavelet or wavelet packet decompositions, the nature of wavelet analysis should be an important factor that determines the robustness of the method. The continuous wavelet analysis is redundant and has tolerance for errors (Daubechies 1997). The discrete wavelet analysis is uniformly converged (Strang and Nguyen) and sufficient for the exact or perfect reconstruction if a wavelet satisfies some admissibility conditions (Daubechies 1997). This provides the robustness for the wavelet or wavelet packet decomposition and reconstruction.

The mapping relationship is based on the comparative tests between the ATD and the human subjects. Therefore, the following factors may also affect the established relationship and thus influences the robustness of the method.

- *Biofidelity of ATD* The method can improve the closeness of a prediction. However, if an ATD lacks essential biofidelity in representing certain human characteristics, reasonable predictions of corresponding human responses are not possible even if the method is utilized.
- *Control of test conditions* In the development of the method, it is assumed that the test conditions except the biomechanics of occupants are controlled to be same for the ATD tests and the human tests. Differences or deviations in these test conditions will impair the common basis on which the comparison between the ATD tests and the human tests is made and thus deteriorate the mapping relationship established.
- *Scope of tests* It can be reasonably assumed that, in each test case, only a particular part of the biomechanics of the occupant (either human or ATD) is excited and exhibited in the response. For a group of tests with different test conditions, different parts of the biomechanics of the occupant may be excited and exhibited. A limited number of tests with limited variations of test conditions may not be able to explore all of the characteristics of the occupant biomechanics, especially if they are considered to be nonlinear in nature, so that both the magnitude and frequency need to be exhausted. Therefore, if the prediction is to be made for a range (interpolation), a chance is that the case to be predicted is related to the parts of the biomechanics of the occupant that have not been explored. In this case, the prediction would be more difficult to make. The chance becomes larger if the prediction is to be made for a case out of range (extrapolation).
- *Sample size* A sufficiently large number of samples or the repeated tests under the same conditions are required for reducing estimation

errors of the mapping matrix. However, for impact tests, a large number of repeated tests are usually neither possible nor feasible.

Impact Range

It is not feasible or even possible to establish a mapping matrix that is able to describe the relationship between the ATD response and the human response for the whole range from non-injury impact to injury impact. Instead, the whole range can be divided into two sub-regions: non-injury region and injury region. In the non-injury region, the relationship can be established based on the data of the tests with ATDs and human volunteers. In the injury region, the data of cadaver tests can be used with the awareness of the differences between the cadaver response and the live human response. In the injury region, structural failure would occur to cadavers, which will be present in the cadaver response usually as abrupt changes. Presumably, the response changes are correlated to the failure pattern. Fortunately, the wavelet analysis is especially suitable for "catching" abrupt changes (singular points) in a signal. Thus the changes will be revealed in the energy distributions based on the wavelet packet decompositions. By comparing the energy distributions of the ATD response and the human response, one can identify those sub-signals due to the structural failure of the cadaver. After proper treatment, these sub-signals can be incorporated when the ATD response is mapped into the corresponding human response.

CONCLUSIONS

Based on wavelet analysis, a methodology has been developed for predicting the human response from ATD tests or for improving the biofidelity of the ATD response. The use of the method in the analysis of a series of side impact tests has shown that the method is effective. Whereas the test data used in the analysis came from low-level, non-injury tests, no restrictions were applied during the method development to confine the method to low-level impact situations. The method can be used in both non-injury and injury impact problems.

The general mapping relationship for a range was established in this study using direct averaging, since only three cases (test cells) were considered in this range. If a range is defined by a number of test cases, a sophisticated statistical analysis is required for establishing the general mapping relationship. The mechanism of automatic accumulation, self-learning, and self-adaptation can be introduced into the process of establishing a mapping relationship to improve its robustness. The use of the method in high-level-impact injury problems may unveil the problems of nonlinearity that need more treatment in the method.

REFERENCES

Bendat, J.S. and Piersol, A.G. (1993) Engineering Applications of Correlation and Spectral Analysis. John Wiley Sons, New York.

Cheng, Z.Q., and Pellettiere, J.A. (2003) Correlation Analysis of Automobile Crash Responses Based on Wavelet Decompositions. Mechanical Systems and Signal Processing 17(6): 1237-1257.

Cheng, Z.Q., Pellettiere, J.A., and Rizer, R.L. (2004) Wavelet-Based Validation Methods and Criteria for Finite Element Automobile Crashworthiness Modeling. Proc. of XXII International Modal Analysis Conference. Society for Experimental Mechanics, Michigan.

Daubechies, I. (1997) Ten Lectures on Wavelets. The Society for Industrial and Applied Mathematics, Pennsylvania.

Kallieris, D., Mattern, R., McIntosh, A., and Boggasch, F. (1992) The Biofidelity of EUROSID 1 and BIOSID. Proc. of 36th Stapp Car Crash Conference. SAE Paper 922518.

Mallat, S. (1998) A Wavelet Tour of Signal Processing. Academic Press.

Misiti, M. and Misiti, Y. (1997) Wavelets Toolbox User's Guide. The MathWorks, Inc., Massachusetts.

Morgan, R.M., Marcus, J.H., and Eppinger, R.H. (1981) Correlation of Side Impact Dummy/Cadaver Tests. Proc. of 25th Stapp Car Crash Conference. SAE Paper 811008.

Oakley, C. (2001) Human Injury Modeling—Capabilities and Limitations. Proc. of 17th International Technical Conference on the Enhanced Safety of Vehicles. Amsterdam, Holland.

Ogden, R.T. (1997) Essential Wavelets for Statistical Applications and Data Analysis. Birkhauser, Boston.

Schneider, L.W, Ricci, L.L., Salloum, M.J., Beebe, M.S., King, A.I., Rouhana, S.W., and Neathery, R.F. (1992) Design and Development of an Advanced ATD Thorax System for Frontal Crash

Environments. Final Report Volumes 1 & 2, U.S. Department of Transportation, National Highway Traffic Safety Administration, DOT HS 808 138.

Seemann, M.R., Muzzy, W.H., and Lustick, L.S. (1986) Comparison of Human and Hybrid III Head and Neck Dynamic Response. Proc. of 30th Stapp Car Crash Conference. SAE Paper 861892.

Strang, G. and Nguyen, T. (1997) Wavelets and Filter Banks. Wellesley-Cambridge Press, Massachusetts.

Viano, D., Fan, A., Ueno, K., Walilko, T., Cavanaugh, J., and King, A. (1995) Biofidelity and injury assessment in Eurosid I and Biosid. Proc. of 39th Stapp Car Crash Conference. SAE paper 952731.

Watkins T. A., and Guccione, S. J. (1992) Scaling Hybrid III and Human Head Kinematic ResponsetoGx, +Gy and +Gz Impact Acceleration. Proc. of 36th Stapp Car Crash Conference. SAE Paper922512.